PROTECTIVE EFFECTS OF MEMANTINE ON HYDROQUINONE TREATED HUMAN RETINAL PIGMENT EPITHELIUM CELLS AND HUMAN RETINAL MÜLLER CELLS

Mohamed Tarek Moustafa[1,2, †], Claudio Ramirez[1, †], Kevin Schneider[1], Shari R. Atilano[1], Gloria Astrid Limb[3], Baruch D. Kuppermann[1], Maria Cristina Kenney[1, *]

*** Address correspondence to:** M. Cristina Kenney, M.D., Ph.D., Gavin Herbert Eye Institute, University of California Irvine, 843 Health Science Road, Hewitt Hall, Room 2028, Irvine CA, 92697, Phone 949-824-7603, Fax 949-824-9626, Email: mkenney@uci.edu

[1]Gavin Herbert Eye Institute, University of California, Irvine, CA, USA.

[2]Ophthalmology Department, Minia University, Minia, Egypt.

[3]Division of Ocular Biology and Therapeutics, UCL Institute of Ophthalmology, London, United Kingdom.

[†] **These authors equally contributed to this article.**

PROPRIETARY INTEREST

M. Tarek Moustafa: No competing financial interests exist.

Claudio Ramirez: No competing financial interests exist.

Kevin Schneider: No competing financial interests exist.

Shari R. Atilano: No competing financial interests exist.

G. Astrid Limb: No competing financial interests exist.

Baruch D. Kuppermann: Consultant to Alcon, Alimera, Allegro, Allergan, Genentech, Glaukos, GSK, Neurotech, Novagali,

	Novartis, Ophthotech, Pfizer, Regeneron, Santen, SecondSight, Teva, ThromboGenics.
M. Cristina Kenney:	No competing financial interests exist.
RUNNING TITLE:	Protective effect of MEM on HQ-treated cells.
WORD COUNT:	3762
FIGURE LEGENDS:	4
REFERENCES:	69
KEY WORD:	Memantine, hydroquinone, retinal cells

ABSTRACT

Purpose:

Memantine (MEM) acts on the glutamatergic system by blocking NMDA glutamate receptors. The role that MEM plays in protecting retinal cells is unknown. Hydroquinone (HQ) is one of the cyto-toxic components in cigarette smoke. In the present study, we tested whether pre-treatment with MEM could protect against the cyto-toxic effects of HQ on human retinal pigment epithelium cells (ARPE-19) and human retinal Müller cells (MIO-M1) *in vitro*.

Methods:

Cells were plated, pre-treated for 6 hours with 30µM of MEM and then exposed for 24 hours to 200 µM, 100 µM, 50 µM and 25 µM of HQ while MEM was still present. Cell viability (CV), reactive oxygen species (ROS), mitochondrial membrane potential (ΔΨm), and lactate dehydrogenase (LDH) release assays were performed.

Results:

HQ-treated cells showed a dose dependent decrease in CV and ΔΨm but an increase in ROS production and LDH levels in both cell lines. MEM pre-treatment reversed the CV in 50 µM, 100 µM and 200 µM doses in ARPE-19 cells and at all HQ concentrations in MIO-M1 cells compared to HQ-treated cultures. ROS production was reversed in all HQ concentrations in both cell lines. ΔΨm was

significantly increased after MEM pre-treatment only in 50 µM HQ concentration for both cell lines. LDH levels were decreased at 50 µM and 25 µM HQ in ARPE-19 and MIO-M1 cells, respectively.

Conclusion:

HQ-induced toxicity is concentration dependent in ARPE-19 and MIO-M1 cultures. MEM exerts protective effects against HQ-induced toxicity on human retinal pigment epithelial and Müller cells *in vitro*.

INTRODUCTION:

Patients with Alzheimer's disease (AD), one of the most common aging diseases, suffer from progressive memory loss and impairments of cognitive function.[1] AD patients are also at risk for developing retinal degeneration and visual complaints.[2, 3] Blanks et al. reported loss of retinal ganglion calls (RGCs) in AD patients,[4] while Kesler et al. showed reduction in the retinal nerve fiber layer thickness.[5] Similarly to AD, the principal risk factor for Age-related Macular Degeneration (AMD) is aging. The accumulation of lipofuscin and extracellular drusen deposits between the basal lamina of the retinal pigment epithelium (RPE) and the inner collagenous layer of the Bruch's membrane are the hallmark for AMD.[6, 7] Both AMD and AD exhibit the similar pathological features of increased oxidative stress and inflammation. In a classic mouse model of AD, it has been shown histologically that the retina has depositions of amyloid-β (Aβ) within the nerve fiber layer (NFL), inner nuclear layer (INL), RGC layer[8, 9] and inner plexiform layer (IPL).[10]

Memantine (MEM) is a N-Methyl-D-aspartate (NMDA) receptor antagonist. Historically, researchers at Eli Lilly first synthesized MEM in hopes of discovering a blood glucose lowering agent,[11] but the compound lacked such activity. In 1972, Merz and coworkers identified the effects of MEM on central nervous system (CNS) activity and reported its potentials in treating Parkinson's disease,

spasticity, cerebrovascular and psychiatric diseases associated with aging.[12-15] MEM improved the symptoms of patients with AD because it prevents apoptosis, decreases deposition of antibodies[16-18] and inhibits microglial activation.[19, 20] In 2003, MEM was approved for treatment of patients with moderate to severe Alzheimer's disease.[21, 22] MEM decreased the levels of gentamycin-induced apoptosis of spiral ganglion cells in Guinea pigs.[23] In the retina, MEM had anti-apoptotic functions that protected RGC in glaucoma[24] and was effective in reduction of retinal nerve fiber layer (RNFL) thinning seen in patients with optic neuritis.[25] In patients with acute anterior ischemic optic neuropathy, systemic MEM improved the best corrected visual acuity. In a mouse model, it has been hypothesized that the MEM protective effects are due in part to decrease of OPA1 and cytochrome *c* release which lowers levels of downstream apoptosis.[26] Other properties of MEM include counteracting damage caused by ischemia/reperfusion in rabbits and rats retinas,[27, 28] preventing ethambutol-induced retinal injury in rats[29], reducing retinal neurodegeneration in the DBA/2J mouse[30], protecting against low-dose glutamate toxicity in a rat model[31] and reversing cytotoxicity of catechol and Benzo(e)Pyrene, (components from cigarette smoke) in human retinal Müller cells and retinal pigment epithelial cells *in vitro* by decreasing apoptosis as measured by lower caspase-3/7 and caspase-9 activities.[32, 33]

Smoking is considered one of the most important risk factors for developing AMD. Smokers have two to three fold higher risk to develop AMD compared to never-smokers.[34] Smoking has an association with both the wet and dry forms of advanced AMD.[35, 36] The risk declines by 6.7% after one year of smoking cessation, and the risk goes down by another 5% if the no-smoking habit continues. Finally, after 10 years of not smoking, an extra 4.2% risk reduction is added.[37, 38]

Inflammation and oxidative stress caused by cigarette smoke are thought to play a role in developing AMD.[39, 40] Chemicals and carcinogens are found in gas-phase smoke and/or the retained tar within cigarettes filters.[41, 42] Hydroquinone (HQ), a semiquinone mixture, is the most common component found in cigarette` tar,[43] with each cigarette filter having up to 155 mg of HQ.[44] In the industrial work place, HQ is found in X-ray films, photographic paper and is used as a reducing agents in most petrochemical and rubber products. Clinically, HQ can be used to treat hyper-pigmented photo-damaged skin.[45]

Even in the absence of direct exposure to the chemical, human urine can contain low parts-per million (PPM) levels of HQ due to exposure to benzene.[46] Surprisingly, increases in plasma and urine HQ levels that are even higher than after 30 minutes of smoking 4 cigarettes, can occur after oral ingestion of wheat products and pears.[47] *In vitro* studies have shown HQ toxicity on retinal and vascular cell cultures.[48-50] Studies with male F344 rats reported nephrotoxicity and

tumorigenicity after HQ exposure.[51, 52] In an experimental animal model of dry AMD, ingestion of HQ causes formation of sub-RPE deposits and thickening of Bruch`s membrane.[53] HQ-induced oxidative stress leads to decreased activity of matrix metalloproteinase 2 (MMP-2),[54] up-regulation of both vascular endothelial growth factor (VEGF) and pigment epithelium-derived factor (PEDF) and down-regulation of monocyte chemoattractant protein 1 (MCP1) both *in vitro* and in a mice model.[55] Reversing the effects of HQ on cultured cells have been studied previously.[32, 56] The zonulae occludentes junctions between RPE cells represent the outer blood retinal barrier. The RPE, which is adjacent to Bruch's membrane, is responsible for light absorption, phagocytosis of photoreceptor outer segments, and maintaining the subretinal space by transporting/secreting ions and mediators between the various retinal layers.[57] Loss of the RPE cells is the early sign of developing AMD. The ARPE-19 cell line has been shown to have similar functional and structural properties of human RPE cells, which makes the cell line valuable for *in vitro* experiments.[58]

Müller cells, often considered the skeleton of the retina, are glial cells that secrete factors essential in maintaining integrity of the blood retinal barrier.[59, 60] Other functions include funneling light through the retina so as to reach photoreceptors[61] and synthesizing retinoic acid.[62] The MIO-M1 cell line, established at Moorfield Institute of Ophthalmology, has been shown by confocal

microscopy to have known markers of Müller cells, including epidermal growth factor receptor (EGF-R), alpha-smooth muscle actin (alpha-SMA), glutamine synthetase, and glial fibrillary acidic protein (GFAP).[63] Therefore, this cell line is very suitable to study the effects of different pharmacological substances on Müller cells *in vitro*.

The aim of this study was to determine if MEM had protective properties against the cytotoxic effects of HQ the human ARPE-19 and MIO-M1 cell lines.

METHODS:

Cell culture:

ARPE-19 cells (ATCC, Manassas, VA;) were cultured in Dulbecco's modified Eagle's medium (DMEM) mixture 1:1 Ham's F-12 medium (Corning – Cellgro, Mediatech, Manassas, VA), containing 10% fetal bovine serum (FBS), penicillin G 100 U/mL, streptomycin sulfate 0.1 mg/mL, gentamicin 10 mg/mL, and amphotericin B 2.5 mg/mL. Serum-free medium was used after cells reached monolayer confluence. Human MIO-M1 cells, obtained from the Department of Cell Biology of the University College, London,[63] were grown in Dulbecco's modified medium 1X with high glucose (DMEM+GlutaMAX; Gibco, Carlsbad, CA). Initially, cells were cultured in 10% FBS and penicillin G 100 U/mL, streptomycin sulfate 0.1 mg/mL, but to keep the cells in the non-proliferating phase, the culture media were changed to 2% FBS. Both cultured ARPE-19 and

MIO-M1 cells were kept under standard incubating conditions: 37ºC and 5% carbon dioxide.

MEM pretreatment:

The ARPE-19 and MIO-M1 cells received six hours pretreatment with MEM 30 µM dissolved in media. This dose was shown in our previous study to have maximum protective effects.[32] A stock concentration of 20 mM of commercially available HQ powder (Sigma Aldrich, Reagent Plus) was made by solubilization in dimethyl sulfoxide (DMSO). Then cells were exposed to HQ at concentrations of 200 µM, 100 µM, 50 µM and 25 µM and incubated another 24 hours at 37ºC. The MEM was present in the media throughout the culture periods. The controls for these experiments include cells treated with the DMSO-equivalent for 200 µM HQ and also untreated cells.

Cell viability assay:

ARPE-19 and MIO-M1 cells (5 X 10^5 cells/well) were plated in 6-well plates for 24 hours and treated as described above. Cells were harvested using trypsin-EDTA 0.2% for 5 minutes, centrifuged for 5 minutes at 1000 rpm, and then resuspended in 1 mL of culture medium. Cell viability was assessed by trypan blue dye-exclusion with an automated ViCell cell viability analyzer (Beckman Coulter, Inc., Fullerton, CA).

Reactive oxygen species (ROS) assay:

The ROS assay, measuring levels of hydrogen peroxide, peroxyl radicals, and peroxynitrite anions, was performed using the fluorescent dye 2´,7´-dichlorodihydrofluorescein diacetate (H_2DCFDA; Invitrogen-Molecular Probes, Eugene, OR).[64] The fluorescent signal was determined using the fluorescent image scanning unit FMBio III (Hitachi Solutions America) with excitation (EX, 550 nm) and emission (EM, 600 nm) filters.

Mitochondrial membrane potential (ΔΨm) assay:

Detection of ΔΨm values was performed using the JC-1 mitochondrial membrane potential detection kit (Biotium, Hayward, CA). JC-1 (5,5´,6,6´-tetrachloro-1,1´,3,3´-tetraethylbenzimidazolyl-carbocyanine-iodide) is a cationic dye that accumulates in the mitochondrial membranes of healthy cells resulting in red fluorescence (590 nm). When ΔΨm levels are reduced in stressed or damaged cells, this leads to accumulation of the JC-1 dye resulting in green fluorescence (530 nm). The ratio of red to green fluorescence is calculated to obtain the changes in ΔΨm. The fluorescent signals were measured with the fluorescent image scanning unit FMBio III (Hitachi Solutions America, San Bruno, CA) set to detect green (EX, 485 nm and EM, 535 nm) and red (EX, 550 nm and EM 600 nm) emissions.

Lactate dehydrogenase cytotoxicity assay:

The lactate dehydrogenase (LDH) assay for detecting necrosis was performed using the LDH Cytotoxicity Assay Kit II (BioVision, Inc., Mountain View, CA) according to the manufacturer's protocol. This kit uses the WST (4-[3-(4-iodophenyl)-2-(4-nitrophenyl)-2H-5-tetrazolio]-1,3-benzene disulfonate) reagent for detection of LDH released from the damaged cells. NADH release from oxidized lactate by LDH reacts with WST that was measured at 450 nm optical density with a BioTek ELx808 absorbance plate reader (BioTek, Winooski, VT).

Markers for ARPE-19 and MIO-M1 cell lines:

To validate our cell lines, we used real time-qPCR (RT-qPCR) to measure expression levels of genes known to be markers for human RPE cells and human retinal Müller cells. Briefly, ARPE-19 and MIO-M1 cells were plated in 6-well plates and RNA isolated using the RNeasy Mini-Extraction kit (Qiagen, Inc., Valencia, CA). The cDNA was synthesized from 100ng of each RNA sample using the SuperScript-VILO cDNA Synthesis Kit (Invitrogen - Life Technologies, Eugene, OR). To analyze for markers of ARPE-19 cells, RT-qPCR was performed using primers (QuantiTect Primer Assay, Qiagen, Inc., Valencia, CA) for Bestrophin1 *(BEST1*, Gene ID 7439, NM_004183)[65]; Cellular Retinaldehyde-Binding Protein-1 (*CRALBP*, Gene ID 6017, NM_000326)[58,65] and Keratin-18 (*KRT18*, Gene ID 3875, NM_000224) a marker for RPE differentiation.[65]

The markers for MIO-M1 cells were Actin, alpha 2, smooth muscle, aorta (*ACTA2*, Gene ID 59, NM_00114945) and Glial Fibrillary Acidic Protein (*GFAP*, Gene ID 2670, NM_002055).[63] However, low levels of *CRALBP* can also be found in Müller cells.[63]

Each of the marker genes were compared to the housekeeper gene Hydroxymethylbilane Synthase (*HMBS*, Gene ID 3145, NM_000190, NM_001024382, NM_001258208, NM_001258209). Then the fold differences between the ARPE-19 cells and MIO-M1 cells were calculated. The samples were run in triplicate and the experiment repeated twice.

The RT-qPCR was performed using Power SYBR green master mix (Applied Biosystems - Life Technologies, Eugene, OR) on a StepOnePlus Q-PCR system (Applied Biosystems - Life Technologies, Eugene, OR). ΔCt values for each marker gene of interest were calculated through normalization to the internal control *HMBS*. ΔΔCt values were obtained through comparison of ARPE19 and MIO-M1 ΔCt values. Folds were calculated with the formula $2^{\Delta\Delta Ct}$.

In ARPE-19 cells, the expression level for *BEST1* was 88-fold higher than for MIO-M1 cells; the *CRALBP* expression levels were 6.4-fold higher in ARPE-19 cells versus MIO-M1 cells. Finally, the ARPE-19 cells also had higher expression of *KRT18* (62-fold) compared to MIO-M1 cells. Multiple attempts using primers from 2 different companies were made to amplify the *RPE65* gene

but the ARPE-19 cells expressed only low level, variable products. This was not surprising since it has been reported that cultured cells hardly ever express the *RPE65* gene, and when it is expressed *in vitro* the peak expression time point is approximately 42 days in culture.[66] The MIO-M1 cells show significantly higher expression levels of the *ACTA2* (3.4-fold) and the *GFAP* (21.6-fold) genes compared to the ARPE-19 cells.

Our findings demonstrate that the ARPE-19 cells had high expression levels for markers (*BEST1, CRALB* and *KRT18*) for this specific cell type. The MIO-M1 cells produce high levels of the Müller cell markers (*ACTA2* and *GFAP*), but also expressed some levels of *CRALBP*, which was expected. These studies thereby validate that our cultures produced markers consistent with RPE and Müller cells.

Statistical analyses:

Data were analyzed with unpaired t-test and one-way ANOVA using the GraphPad Prism version 5.00 for Windows (GraphPad Software, San Diego, CA; www.graphpad.com). $P \leq 0.05$ (*) statistically significant; $P \leq 0.01$ (**) very significant; $P \leq 0.001$ (***) extremely significant. Error bars in the graphs represent SEM for the triplicate performed experiments.

RESULTS:

Cell viability (CV) studies:

For ARPE-19 cells, the mean percentage cell viability values were 17.03 ± 1.18, 59.43 ± 0.54, 74.57 ± 2 and 94.57 ± 1.16 for 200 µM, 100 µM, 50 µM and 25 µM HQ, respectively, compared to 96.23 ± 1.75 for the DMSO-equivalent (amount of DMSO in the 200 µM HQ sample) (Table 1). Pretreatment with 30 µM MEM resulted in an increase in CV for the 200 µM HQ (54.57 ± 1.83, p = 0.0003), 100 µM HQ (89.53 ± 1.64, p = 0.005) and 50 µM, (92.17 ± 0.67, p = 0.006) when compared to the DMSO-equivalent cultures (Fig. 1a). The 25 µM HQ-treated cultures were not changed (97.27 ± 0.71, p = 0.28).

In MIO-M1 cells, the mean percentage cell viability values for 200 µM, 100 µM, 50 µM and 25 µM HQ-treated MIO-M1 cells were 31.83 ± 0.32, 36.27 ± 0.65, 61.07 ± 0.49 and 89.30 ± 0.3 respectively, compared to 91.33 ± 0.7 at DMSO-equivalent cultures. The cell viability values were increased after MEM pretreatment at all concentrations: 200 µM had 83.73 ± 2.42 (p = 0.002); 100 µM had 83.27 ± 1.3 (p = 0.0002); 50 µM had 84.17 ± 2.04 (p = 0.012) and 25µ M HQ was 90.40 ± 0.06 (p = 0.049) compared to the HQ-alone treated samples (Fig. 1b).

ROS assay

In ARPE-19 cell line, ROS production levels were increased after HQ treatment with relative fluorescence values (RFV) of 13733 ± 759.3, 13377 ± 622.6, 11932 ± 367.7 and 10344 ± 388.3 for HQ at 200 µM, 100 µM, 50 µM and

25 µM concentrations, respectively compared to the DMSO-equivalent value of 3807 ± 258.2 (Fig. 2a) (Table 2). The ROS levels were decreased significantly with MEM pretreatment for all of the HQ-treated cultures. The RFV was 9469 ± 876.8 ($p = 0.0026$) at 200 µM, 5710 ± 938.0 ($p = 0.002$) at 100 µM, 3986 ± 838.2 ($p = 0.006$) at 50 µM and 3566 ± 447.2 ($p = 0.01$) at 25 µM of HQ + MEM treated cultures (Fig. 2a).

Similar protective effects by MEM were found in MIO-M1 cells treated with varying concentrations of HQ (Fig. 2b). The relative fluorescence values of 13369 ± 396.5 for 200 µM HQ-treated, 11377 ± 83.14 for 100 µM HQ-treated, 10266 ± 102.5 at 50 µM HQ-treated and 9977 ± 89.63 at 25 µM HQ-treated compared to the DMSO-equivalent cultures with the RFV of 3421 ± 48.42. These values were significantly decreased after MEM pretreatment at all concentrations; the values were 8036 ± 618.4 ($p = 0.004$), 5043 ± 739.5, ($p = 0.011$), 3599 ± 431.7 ($p = 0.003$) and 3232 ± 113.9 ($p = 0.0001$) for MEM plus 200 µM, 100 µM, 50 µM and 25 µM of HQ, respectively (Fig. 2b).

Mitochondrial membrane potential assay

The $\Delta\Psi m$ fluorescence ratios in the ARPE-19 cells exposed to 200 µM, 100 µM, 50 µM or 25 µM of HQ were 3654 ± 71.73, 3941 ± 77.02, 5167 ± 33.32 and 7543 ± 78.03, respectively compared to the DMSO-equivalent treated cells (9180 ±

75.62, Fig 3a) (Table 3). These values were corrected only at 50 µM HQ-treated cells after 6 hours of MEM pretreatment with value of 6951 ± 58.74 ($p = 0.0006$) when compared to the HQ-equivalent value. The other MEM treated samples did not show significant changes in ΔΨm fluorescence levels compared to the HQ-treated counterparts; MEM + 200 µM HQ-treated at 3713 ± 61.36 ($p = 0.17$), MEM + 100 µM HQ-treated at 4112 ± 99.83 ($p = 0.43$) and MEM + 25 µM HQ-treated at 7517 ± 46.67 ($p = 0.49$) (Fig.3a).

ΔΨm fluorescence ratios for MIO-M1 cells treated with 200 µM, 100 µM, 50 µM or 25 µM of HQ alone were 3104 ± 85.34, 4420 ± 59.60, 5626 ± 53.41 and 7673 ± 70.50, respectively compared to the DMSO-equivalent cells (9154 ± 82.10). As was seen in ARPE-19 cell line, the fluorescence ratio of only the 50 µM HQ + MEM cultures were increased to 6729 ± 74.14 ($p = 0.0005$) compared to its HQ-treated values. The other values were not significantly changed; for the MEM + 200µM HQ-treated values (3099 ± 93.06, $p = 0.61$), MEM + 100 µM HQ-treated values (4390 ± 41.31, $p = 0.74$) and MEM + 25 µM HQ-treated (7740 ± 54.61, $p = 0.52$) compared to the HQ-treated counterparts (Fig. 3b).

LDH release assay

Conditioned media of ARPE-19 cells treated with 200 µM, 100 µM, 50 µM or 25 µM of HQ alone showed LDH levels of 5.4 ± 0.067, 4.7 ± 0.088, 4.1 ± 0.049

and 2.1 ± 0.13, respectively, compared to the DMSO-equivalent treated cells, 1.6 ± 0.06 (Table 4). The LDH levels were decreased significantly in the MEM + 50 µM HQ cultures (2.3 ± 0.036, p = 0.002). However, the values for the other samples were not significantly changed; values for MEM + 200 µM HQ-treated were 5.4 ± 0.23 (p = 0.8), MEM + 100 µM HQ-treated showed 4.6 ± 0.034 (p = 0.8) and MEM + 25 µM HQ-treated was 1.5 ± 0.13 (p = 0.1) compared to the HQ-alone samples (Fig. 4a).

Conditioned media of MIO-M1 cells treated with different concentrations of HQ alone showed LDH levels of 6.1 ± 0.058, 5.7 ± 0.043, 5.3 ± 0.041 and 2.1 ± 0.013 for 200 µM, 100 µM, 50 µM or 25 µM, respectively, compared to the DMSO-equivalent treated cells (1.2 ± 0.058). The levels of LDH decreased significantly after pretreatment with MEM only at the 25 µM HQ-treated cultures (1.2 ± 0.076, p = 0.006). The MEM + 200 µM, MEM + 100 µM and MEM + 50 µM HQ values (56.1 ± 0.035, p = 0.42); 5.5 ± 0.13, p = 0.57; and 5.2 ± 0.022, p = 0.32, respectively) were not significantly different from the HQ-treated (Fig. 4b).

DISCUSSION

Previous studies have shown that HQ had toxic effects on cultured human RPE cells (ARPE-19)[49, 56], human Müller retinal cells (MIO-M1),[50, 56] human microvascular endothelial cells and rat neurosensory retinal cells (R-28).[49] The

present study demonstrates that MEM has dose-dependent protective properties in human ARPE-19 and MIO-M1 cells that were stressed with HQ. Previously, Mansoor et. al., reported that MEM had anti-apoptotic effects and decreased the ROS production after treating with catechol and Benzo(e)Pyrene, components from cigarette smoke, on cultured ARPE-19[33] and Mùller cells.[32] MEM was also been shown to be beneficial in other ocular cells *in vitro*. For example, a glaucoma study showed MEM provided protection against RGCs death.[24, 67]

Clinical studies with patients have reported the therapeutic effects of MEM in aging patients with neuro-psychiatric diseases are through anti-apoptosis, decreasing extracellular deposition of fibrillogenic amyloid-beta peptides (Abeta)[16-18] and inhibiting of microglial activation.[19, 20]

In our study, both ARPE-19 and MIO-M1 cells showed increased cell viabilities at all concentrations of HQ after pretreatment with MEM. The largest reversals of CV were seen in the ARPE-19 cell cultures treated with 200 µM HQ (17.03% to 54.57%), and in MIO-M1 cell cultures treated with 100 µM HQ (36.27% to 83.27%). Since smoking is the most common reversible risk factor for developing AMD, and HQ is a major component of smoking, then it may be reasonable to use MEM in those AMD patients that are unable to quit and still smoking.

MEM successfully reversed in both cell lines the elevated ROS levels induced by HQ-treatment. This demonstrated that HQ stimulated the oxidative stress pathway[56] but MEM could block it. In contrast, MEM was not successful in reversing the HQ-induced decline in $\Delta\Psi m$, as seen by the fact that only at the single dose of 50 µM HQ were the ARPE-19 or MIO-M1 cells protected by MEM. This suggests that MEM`s effects were greater at blocking ROS production and less at providing stability to the mitochondrial membrane potential.

LDH production reflects the degree of necrosis in cultured cells. In ARPE-19 and MIO-M1 cells, the HQ treatment induced an increase of LDH levels in a dose-dependent manner. It was only at the lower HQ concentrations (50 µM HQ for ARPE-19 and 25 µM for MIO-M1) that MEM pre-treatment had any protective effects, (LDH levels decrease in ARPE-19 cultures from 4.1 ± 0.049 to 2.3 ± 0.36; MIO-M1 had decreased levels from 2.1 ± 0.013 to 1.2 ± 0.076). These results demonstrate that the degree of necrosis and cell damage resulting from HQ toxicity can only be slightly reversed by pre-treatment with MEM. Danuta et al., showed that MEM attenuated the staurosporine-induced activation of caspase-3 and LDH release in hippocampal cultured neurons, moderately inhibited LDH only in striatal culture and partially inhibited staurosporine-induced neuronal injury in neocortical cultures.[68]

There have been only a limited number of studies to identify potential drugs capable of reversing HQ toxicity. It was shown in ARPE-19 and MIO-M1 cells that Brimonidine exhibited protective properties against the HQ toxicity by increasing the cell viability and mitochondrial membrane potential, while decreasing the LDH and ROS levels.[56] However, to date no other inhibitors have been reported that block the HQ cyto-toxic effects.

A limitation to our study is the use of transformed cell lines (ARPE-19 and MIO-M1) to address retinal biology because these cultures can be very different from the non-transformed retinal cells. Using array analyses, Tian et al showed that ARPE-19 cells have different gene expression profiles than the native RPE cells and the patterns can be modulated by varying the substrates and serum levels.[69] Therefore, while valuable information can be gained from ARPE-19 studies, future studies are needed to validate the protective effects of MEM using RPE cells grown on transwell inserts that have developed physiological polarity and cultured primary cells.

In summary, our results demonstrate that (1) HQ-induced toxicity is directly proportion to the concentration used; (2) HQ toxicity is mediated through multiple pathways including, mitochondrial membrane alteration, oxidative stress and the necrosis pathway; (3) MEM can protect both human RPE cells and Müller cells from HQ-induced damage through lowering ROS production levels and to a lesser

extend through stabilization of the mitochondrial membrane potential. Future studies should include evaluation of MEM`s protective effects in the *in vivo* models for a better understanding of the potential uses of this drug.

REPRINT REQUESTS SHOULD BE DIRECTED TO:

M. Cristina Kenney, M.D., Ph.D.,

Phone 949-824-7603,

Fax 949-824-9626,

Email: mkenney@uci.edu

AUTHOR DISCLOSURE STATEMENT:

M. Tarek Moustafa:	No competing financial interests exist.
Claudio Ramirez:	No competing financial interests exist.
Kevin Schneider:	No competing financial interests exist.
Shari R. Atilano:	No competing financial interests exist.
G. Astrid Limb:	No competing financial interests exist.
Baruch D. Kuppermann:	Consultant to Alcon, Alimera, Allegro, Allergan, Genentech, Glaukos, GSK, Neurotech, Novagali, Novartis, Ophthotech, Pfizer, Regeneron, Santen, SecondSight, Teva, ThromboGenics.
M. Cristina Kenney:	No competing financial interests exist.

REFERENCES:

1. Fan X, Sun D, Tang X, Cai Y, Yin ZQ, Xu H. Stem-cell challenges in the treatment of Alzheimer's disease: a long way from bench to bedside. *Med Res Rev*. 2014; 34:957-978.
2. Bayer AU, Ferrari F, Erb C. High occurrence rate of glaucoma among patients with Alzheimer's disease. *Eur Neurol*. 2002; 47:165-168.
3. Guo L, Duggan J, Cordeiro MF. Alzheimer's disease and retinal neurodegeneration. *Curr Alzheimer Res*. 2010; 7:3-14.
4. Blanks JC, Torigoe Y, Hinton DR, Blanks RH. Retinal pathology in Alzheimer's disease. I. Ganglion cell loss in foveal/parafoveal retina. *Neurobiol Aging*. 1996; 17:377-384.
5. Kesler A, Vakhapova V, Korczyn AD, Naftaliev E, Neudorfer M. Retinal thickness in patients with mild cognitive impairment and Alzheimer's disease. *Clin Neurol Neurosurg*. 2011; 113:523-526.
6. Donoso LA, Kim D, Frost A, Callahan A, Hageman G. The role of inflammation in the pathogenesis of age-related macular degeneration. *Surv Ophthalmol*. 2006; 51:137-152.
7. Curcio CA, Johnson M, Huang JD, Rudolf M. Aging, age-related macular degeneration, and the response-to-retention of apolipoprotein B-containing lipoproteins. *Prog Retin Eye Res*. 2009; 28:393-422.
8. Dutescu RM, Li QX, Crowston J, Masters CL, Baird PN, Culvenor JG. Amyloid precursor protein processing and retinal pathology in mouse models of Alzheimer's disease. *Graefes Arch Clin Exp Ophthalmol*. 2009; 247:1213-1221.
9. Ning A, Cui J, To E, Ashe KH, Matsubara J. Amyloid-beta deposits lead to retinal degeneration in a mouse model of Alzheimer disease. *Invest Ophthalmol Vis Sci*. 2008; 49:5136-5143.
10. Perez SE, Lumayag S, Kovacs B, Mufson EJ, Xu S. Beta-amyloid deposition and functional impairment in the retina of the APPswe/PS1DeltaE9 transgenic mouse model of Alzheimer's disease. *Invest Ophthalmol Vis Sci*. 2009; 50:793-800.
11. Gerzon K, Krumkalns EV, Brindle RL, Marshall FJ, Root MA. The Adamantyl Group in Medicinal Agents. I. Hypoglycemic N-Arylsulfonyl-N' -Adamantylureas. *J Med Chem*. 1963; 6:760-763.
12. Grossmann W, Schutz W. [Memantine and neurogenic bladder disorders within the bounds of spastic conditions]. *Arzneimittelforschung*. 1982; 32:1273-1276.
13. Miltner FO. [Valve of symptomatic therapy with memantine in cerebral coma. II. Development of stretch synergisms in coma with brain stem symptoms]. *Arzneimittelforschung*. 1982; 32:1271-1273.
14. Schneider E, Fischer PA, Clemens R, Balzereit F, Funfgeld EW, Haase HJ. [Effects of oral memantine administration on Parkinson symptoms. Results of a placebo-controlled multicenter study]. *Dtsch Med Wochenschr*. 1984; 109:987-990.
15. Mundinger F, Milios E. [Experiences with memantine in the treatment of severe spastic and extrapyramidal movement disorders in combination with stereotaxic surgery]. *Nervenarzt*. 1985; 56:106-109.
16. Bormann J. Memantine is a potent blocker of N-methyl-D-aspartate (NMDA) receptor channels. *Eur J Pharmacol*. 1989; 166:591-592.
17. Hare WA, Wheeler L. Experimental glutamatergic excitotoxicity in rabbit retinal ganglion cells: block by memantine. *Invest Ophthalmol Vis Sci*. 2009; 50:2940-2948.
18. Alley GM, Bailey JA, Chen D, Ray B, Puli LK, Tanila H, Banerjee PK, Lahiri DK. Memantine lowers amyloid-beta peptide levels in neuronal cultures and in APP/PS1 transgenic mice. *J Neurosci Res*. 2010; 88:143-154.

19. Sun D, Chen J, Bao X, Cai Y, Zhao J, Huang J, Huang W, Fan X, Xu H. Protection of Radial Glial-Like Cells in the Hippocampus of APP/PS1 Mice: a Novel Mechanism of Memantine in the Treatment of Alzheimer's Disease. *Mol Neurobiol*. 2015; 52:464-477.
20. Wu HM, Tzeng NS, Qian L, Wei SJ, Hu X, Chen SH, Rawls SM, Flood P, Hong JS, Lu RB. Novel neuroprotective mechanisms of memantine: increase in neurotrophic factor release from astroglia and anti-inflammation by preventing microglial activation. *Neuropsychopharmacology*. 2009; 34:2344-2357.
21. Rabey JM, Nissipeanu P, Korczyn AD. Efficacy of memantine, an NMDA receptor antagonist, in the treatment of Parkinson's disease. *J Neural Transm Park Dis Dement Sect*. 1992; 4:277-282.
22. Gauthier S, Herrmann N, Ferreri F, Agbokou C. Use of memantine to treat Alzheimer's disease. *CMAJ*. 2006; 175:501-502.
23. Kim BY, Bae WY, Hur DY, Kim JR, Koh TK, Lee TH, Park GB. Effects of Memantine on Aminoglycoside-Induced Apoptosis of Spiral Ganglion Cells in Guinea Pigs. *Otolaryngol Head Neck Surg*. 2016; 155:147-154.
24. Lipton SA. Possible role for memantine in protecting retinal ganglion cells from glaucomatous damage. *Surv Ophthalmol*. 2003; 48 Suppl 1:S38-46.
25. Esfahani MR, Harandi ZA, Movasat M, Nikdel M, Adelpour M, Momeni A, Merat H, Fard MA. Memantine for axonal loss of optic neuritis. *Graefes Arch Clin Exp Ophthalmol*. 2012; 250:863-869.
26. Ju WK, Kim KY, Angert M, Duong-Polk KX, Lindsey JD, Ellisman MH, Weinreb RN. Memantine blocks mitochondrial OPA1 and cytochrome c release and subsequent apoptotic cell death in glaucomatous retina. *Invest Ophthalmol Vis Sci*. 2009; 50:707-716.
27. Osborne NN. Memantine reduces alterations to the mammalian retina, in situ, induced by ischemia. *Vis Neurosci*. 1999; 16:45-52.
28. Yigit U, Erdenoz S, Uslu U, Oba E, Cumbul A, Cagatay H, Aktas S, Eskicoglu E. An immunohistochemical analysis of the neuroprotective effects of memantine, hyperbaric oxygen therapy, and brimonidine after acute ischemia reperfusion injury. *Molecular vision*. 2011; 17:1024-1033.
29. Abdel-Hamid AA, Firgany Ael D, Ali EM. Effect of memantine: A NMDA receptor blocker, on ethambutol-induced retinal injury. *Annals of anatomy = Anatomischer Anzeiger : official organ of the Anatomische Gesellschaft*. 2016; 204:86-92.
30. Atorf J, Scholz M, Garreis F, Lehmann J, Brauer L, Kremers J. Functional protective effects of long-term memantine treatment in the DBA/2J mouse. *Documenta ophthalmologica. Advances in ophthalmology*. 2013; 126:221-232.
31. Vorwerk CK, Lipton SA, Zurakowski D, Hyman BT, Sabel BA, Dreyer EB. Chronic low-dose glutamate is toxic to retinal ganglion cells. Toxicity blocked by memantine. *Invest Ophthalmol Vis Sci*. 1996; 37:1618-1624.
32. Mansoor S, Gupta N, Luczy-Bachman G, Limb GA, Kuppermann BD, Kenney MC. Protective effects of memantine and epicatechin on catechol-induced toxicity on Muller cells in vitro. *Toxicology*. 2010; 271:107-114.
33. Mansoor S, Gupta N, Patil AJ, Estrago-Franco MF, Ramirez C, Migon R, Sapkal A, Kuppermann BD, Kenney MC. Inhibition of apoptosis in human retinal pigment epithelial cells treated with benzo(e)pyrene, a toxic component of cigarette smoke. *Invest Ophthalmol Vis Sci*. 2010; 51:2601-2607.
34. Thornton J, Edwards R, Mitchell P, Harrison RA, Buchan I, Kelly SP. Smoking and age-related macular degeneration: a review of association. *Eye (Lond)*. 2005; 19:935-944.

35. Age-Related Eye Disease Study Research G. Risk factors associated with age-related macular degeneration. A case-control study in the age-related eye disease study: Age-Related Eye Disease Study Report Number 3. *Ophthalmology*. 2000; 107:2224-2232.
36. Clemons TE, Milton RC, Klein R, Seddon JM, Ferris FL, 3rd, Age-Related Eye Disease Study Research G. Risk factors for the incidence of Advanced Age-Related Macular Degeneration in the Age-Related Eye Disease Study (AREDS) AREDS report no. 19. *Ophthalmology*. 2005; 112:533-539.
37. Neuner B, Wellmann J, Dasch B, Behrens T, Claes B, Dietzel M, Pauleikhoff D, Hense HW. Modeling smoking history: a comparison of different approaches in the MARS study on age-related maculopathy. *Ann Epidemiol*. 2007; 17:615-621.
38. Chew EY, Clemons TE, Agron E, Sperduto RD, Sangiovanni JP, Davis MD, Ferris FL, 3rd, Age-Related Eye Disease Study Research G. Ten-year follow-up of age-related macular degeneration in the age-related eye disease study: AREDS report no. 36. *JAMA Ophthalmol*. 2014; 132:272-277.
39. Cascella R, Ragazzo M, Strafella C, Missiroli F, Borgiani P, Angelucci F, Marsella LT, Cusumano A, Novelli G, Ricci F, Giardina E. Age-related macular degeneration: insights into inflammatory genes. *J Ophthalmol*. 2014; 2014:582842.
40. Chiras D, Kitsos G, Petersen MB, Skalidakis I, Kroupis C. Oxidative stress in dry age-related macular degeneration and exfoliation syndrome. *Crit Rev Clin Lab Sci*. 2015; 52:12-27.
41. Talhout R, Schulz T, Florek E, van Benthem J, Wester P, Opperhuizen A. Hazardous compounds in tobacco smoke. *Int J Environ Res Public Health*. 2011; 8:613-628.
42. World Health O. WHO STUDY GROUP ON TOBACCO PRODUCT REGULATION. Report on the Scientific Basis of Tobacco Product Regulations: Fifth Report of a WHO Study Group. *World Health Organ Tech Rep Ser*. 2015:1-234, back cover.
43. Pryor WA. Cigarette smoke radicals and the role of free radicals in chemical carcinogenicity. *Environ Health Perspect*. 1997; 105 Suppl 4:875-882.
44. Bolton JL, Trush MA, Penning TM, Dryhurst G, Monks TJ. Role of quinones in toxicology. *Chem Res Toxicol*. 2000; 13:135-160.
45. Draelos ZD. Novel approach to the treatment of hyperpigmented photodamaged skin: 4% hydroquinone/0.3% retinol versus tretinoin 0.05% emollient cream. *Dermatol Surg*. 2005; 31:799-804.
46. Bechtold WE, Sun JD, Birnbaum LS, Yin SN, Li GL, Kasicki S, Lucier G, Henderson RF. S-phenylcysteine formation in hemoglobin as a biological exposure index to benzene. *Arch Toxicol*. 1992; 66:303-309.
47. Deisinger PJ, Hill TS, English JC. Human exposure to naturally occurring hydroquinone. *J Toxicol Environ Health*. 1996; 47:31-46.
48. Patil AJ, Gramajo AL, Sharma A, Seigel GM, Kuppermann BD, Kenney MC. Differential effects of nicotine on retinal and vascular cells in vitro. *Toxicology*. 2009; 259:69-76.
49. Sharma A, Patil JA, Gramajo AL, Seigel GM, Kuppermann BD, Kenney CM. Effects of hydroquinone on retinal and vascular cells in vitro. *Indian J Ophthalmol*. 2012; 60:189-193.
50. Ramirez C, Pham K, Franco MF, Chwa M, Limb A, Kuppermann BD, Kenney MC. Hydroquinone induces oxidative and mitochondrial damage to human retinal Muller cells (MIO-M1). *Neurotoxicology*. 2013; 39:102-108.
51. National Toxicology P. NTP Toxicology and Carcinogenesis Studies of Hydroquinone (CAS No. 123-31-9) in F344/N Rats and B6C3F1 Mice (Gavage Studies). *Natl Toxicol Program Tech Rep Ser*. 1989; 366:1-248.

52. Shibata MA, Hirose M, Tanaka H, Asakawa E, Shirai T, Ito N. Induction of renal cell tumors in rats and mice, and enhancement of hepatocellular tumor development in mice after long-term hydroquinone treatment. *Jpn J Cancer Res*. 1991; 82:1211-1219.
53. Espinosa-Heidmann DG, Suner IJ, Catanuto P, Hernandez EP, Marin-Castano ME, Cousins SW. Cigarette smoke-related oxidants and the development of sub-RPE deposits in an experimental animal model of dry AMD. *Invest Ophthalmol Vis Sci*. 2006; 47:729-737.
54. Alcazar O, Cousins SW, Marin-Castano ME. MMP-14 and TIMP-2 overexpression protects against hydroquinone-induced oxidant injury in RPE: implications for extracellular matrix turnover. *Invest Ophthalmol Vis Sci*. 2007; 48:5662-5670.
55. Pons M, Marin-Castano ME. Cigarette smoke-related hydroquinone dysregulates MCP-1, VEGF and PEDF expression in retinal pigment epithelium in vitro and in vivo. *PLoS One*. 2011; 6:e16722.
56. Ramirez C, Caceres-Del-Carpio J, Chu J, Chu J, Moustafa MT, Chwa M, Limb GA, Kuppermann BD, Kenney MC. Brimonidine Can Prevent In Vitro Hydroquinone Damage on Retinal Pigment Epithelium Cells and Retinal Muller Cells (MIO-M1). *J Ocul Pharmacol Ther*. 2015.
57. Strauss O. The retinal pigment epithelium in visual function. *Physiol Rev*. 2005; 85:845-881.
58. Dunn KC, Aotaki-Keen AE, Putkey FR, Hjelmeland LM. ARPE-19, a human retinal pigment epithelial cell line with differentiated properties. *Exp Eye Res*. 1996; 62:155-169.
59. Sarthy PV, Lam DM. Biochemical studies of isolated glial (Muller) cells from the turtle retina. *J Cell Biol*. 1978; 78:675-684.
60. Constable PA, Lawrenson JG. Glial cell factors and the outer blood retinal barrier. *Ophthalmic Physiol Opt*. 2009; 29:557-564.
61. Franze K, Grosche J, Skatchkov SN, Schinkinger S, Foja C, Schild D, Uckermann O, Travis K, Reichenbach A, Guck J. Muller cells are living optical fibers in the vertebrate retina. *Proc Natl Acad Sci U S A*. 2007; 104:8287-8292.
62. Edwards RB, Adler AJ, Dev S, Claycomb RC. Synthesis of retinoic acid from retinol by cultured rabbit Muller cells. *Exp Eye Res*. 1992; 54:481-490.
63. Limb GA, Salt TE, Munro PM, Moss SE, Khaw PT. In vitro characterization of a spontaneously immortalized human Muller cell line (MIO-M1). *Invest Ophthalmol Vis Sci*. 2002; 43:864-869.
64. Chwa M, Atilano SR, Reddy V, Jordan N, Kim DW, Kenney MC. Increased stress-induced generation of reactive oxygen species and apoptosis in human keratoconus fibroblasts. *Invest Ophthalmol Vis Sci*. 2006; 47:1902-1910.
65. Burke JM. Epithelial phenotype and the RPE: is the answer blowing in the Wnt? *Prog Retin Eye Res*. 2008; 27:579-595.
66. Alizadeh M, Wada M, Gelfman CM, Handa JT, Hjelmeland LM. Downregulation of differentiation specific gene expression by oxidative stress in ARPE-19 cells. *Invest Ophthalmol Vis Sci*. 2001; 42:2706-2713.
67. Gao Y, Hu YZ, Li RS, Han ZT, Geng Y, Xia Z, Du WJ, Liu LX, Zhang HH, Wang LN. Cattle encephalon glycoside and ignotin injection improves cognitive impairment in APPswe/PS1dE9 mice used as multitarget anti-Alzheimer's drug candidates. *Neuropsychiatric disease and treatment*. 2015; 11:537-548.
68. Jantas-Skotniczna D, Kajta M, Lason W. Memantine attenuates staurosporine-induced activation of caspase-3 and LDH release in mouse primary neuronal cultures. *Brain research*. 2006; 1069:145-153.
69. Tian J, Ishibashi K, Honda S, Boylan SA, Hjelmeland LM, Handa JT. The expression of native and cultured human retinal pigment epithelial cells grown in different culture conditions. *Br J Ophthalmol*. 2005; 89:1510-1517.

FIGURE LEGENDS:

Moustafa. Fig. 1. Cell viability assay. (**A**) ARPE-19 cells treated with 25 μM, 50 μM, 100 μM and 200 μM of HQ with or without 30 μM of MEM. (**B**) MIO-M1 cells treated with 25 μM, 50 μM, 100 μM and 200 μM of HQ with or without 30 μM of MEM.

Moustafa. Fig. 2: Reactive oxygen species (ROS) production assay. (**A**) ARPE-19 cells treated with 25 μM, 50 μM, 100 μM and 200 μM of HQ with or without 30 μM of MEM. (**B**) MIO-M1 cells treated with 25 μM, 50 μM, 100 μM and 200 μM of HQ with or without 30 μM of MEM.

Moustafa. Fig. 3: Mitochondrial membrane potential (ΔΨm) assay. (**A**) ARPE-19 cells treated with 25 μM, 50 μM, 100 μM and 200 μM of HQ with or without 30 μM of MEM. (**B**) MIO-M1 cells treated with 25 μM, 50 μM, 100 μM and 200 μM of HQ with or without 30 μM of MEM.

Moustafa. Fig. 4: Lactate dehydrogenase (LDH) release assay. (**A**) ARPE-19 cells treated with 25 μM, 50 μM, 100 μM and 200 μM of HQ with or without 30 μM of MEM. (**B**) MIO-M1 cells treated with 25 μM, 50 μM, 100 μM and 200 μM of HQ with or without 30 μM of MEM.

TABLE LEGENDS:

Moustafa. Table 1: Results for the cell viability assay showing percentage of cell viability with 25 μM, 50 μM, 100 μM and 200 μM of HQ with or without 30 μM of MEM in both cell lines.

Moustafa. Table 2: Results for the ROS assay showing values of relative fluorescence with 25 μM, 50 μM, 100 μM and 200 μM of HQ with or without 30 μM of MEM in both cell lines.

Moustafa. Table 3: Results for the mitochondrial membrane potential assay showing values of fluorescence ratio with 25 μM, 50 μM, 100 μM and 200 μM of HQ with or without 30 μM of MEM in both cell lines.

Moustafa. Table 4: Results for the LDH release assay showing LDH levels with 25 μM, 50 μM, 100 μM and 200 μM of HQ with or without 30 μM of MEM in both cell lines.

	ARPE-19		**MIO-M1**	
DMSO-equivalent to the 200 µM HQ sample.	96.23 ± 1.75		91.33 ± 0.7	
200 µM HQ	**No MEM**	**Pretreatment with 30 µM MEM**	**No MEM**	**Pretreatment with 30 µM MEM**
	17.03 ± 1.18	54.57 ± 1.83 p = 0.0003	31.83 ± 0.32	83.73 ± 2.42 p = 0.002
100 µM HQ	59.43 ± 0.54	89.53 ± 1.64 p = 0.005	36.27 ± 0.65	83.27 ± 1.3 p = 0.0002
50 µM HQ	74.57 ± 2	92.17 ± 0.67 p = 0.006	61.07 ± 0.49	84.17 ± 2.04 p = 0.012
25 µM HQ	94.57 ± 1.16	97.27 ± 0.71 p = 0.28	89.30 ± 0.3	90.40 ± 0.06 p = 0.049

Table 1 Results for the cell viability assay showing percentage of cell viability with 25 µM, 50 µM, 100 µM and 200 µM of HQ with or without 30 µM of MEM in both cell lines.

	ARPE-19		**MIO-M1**	
DMSO-equivalent to the 200 µM HQ sample.	3807 ± 258.2		3421 ± 48.42	
200 µM HQ	**No MEM**	**Pretreatment with 30 µM MEM**	**No MEM**	**Pretreatment with 30 µM MEM**
	13733 ± 759.3	9469 ± 876.8 p = 0.0026	13369 ± 396.5	8036 ± 618.4 p = 0.004
100 µM HQ	13377 ± 622.6	5710 ± 938 p = 0.002	11377 ± 83.14	5043 ± 739.5 p = 0.011
50 µM HQ	11932 ± 367.7	3986 ± 838.2 p = 0.006	10266 ± 102.5	3599 ± 431.7 p = 0.003
25 µM HQ	10344 ± 388.3	3566 ± 447.2 p = 0.01	9977 ± 89.63	3232 ± 113.9 p = 0.0001

Table 2 Results for the ROS assay showing values of relative fluorescence with 25 µM, 50 µM, 100 µM and 200 µM of HQ with or without 30 µM of MEM in both cell lines.

	ARPE-19		MIO-M1	
DMSO-equivalent to the 200 µM HQ sample.	9180 ± 75.62		9154 ± 82.10	
200 µM HQ	**No MEM**	**Pretreatment with 30 µM MEM**	**No MEM**	**Pretreatment with 30 µM MEM**
	3654 ± 71.73	3713 ± 61.36 p = 0.17	3104 ± 85.34	3099 ± 93.06 p = 0.61
100 µM HQ	3941 ± 77.02	4112 ± 99.83 p = 0.43	4420 ± 59.60	4390 ± 41.3 p = 0.74
50 µM HQ	5167 ± 33.32	6951 ± 58.74 p = 0.0006	5626 ± 53.41	6729 ± 74.14 p = 0.0005
25 µM HQ	7543 ± 78.03	7517 ± 46.67 p = 0.49	7673 ± 70.50	7740 ± 54.6 p = 0.52

Table 3 Results for the mitochondrial membrane potential assay showing values of fluorescence ratio with 25 µM, 50 µM, 100 µM and 200 µM of HQ with or without 30 µM of MEM in both cell lines.

	ARPE-19		**MIO-M1**	
DMSO-equivalent to the 200 µM HQ sample.	1.6 ± 0.06		1.2 ± 0.058	
200 µM HQ	**No MEM**	**Pretreatment with 30 µM MEM**	**No MEM**	**Pretreatment with 30 µM MEM**
	5.4 ± 0.067	5.4 ± 0.23 p = 0.8	6.1 ± 0.058	56.1 ± 0.035 p = 0.42
100 µM HQ	4.7 ± 0.088	4.6 ± 0.034 p = 0.8	5.7 ± 0.043	5.5 ± 0.13 p = 0.57
50 µM HQ	4.1 ± 0.049	2.3 ± 0.036 p = 0.002	5.3 ± 0.041	5.2 ± 0.022 p = 0.32
25 µM HQ	2.1 ± 0.13	1.5 ± 0.13 p = 0.1	2.1 ± 0.013	1.2 ± 0.076 p = 0.006

Table 4 Results for the LDH release assay showing LDH levels with 25 µM, 50 µM, 100 µM and 200 µM of HQ with or without 30 µM of MEM in both cell lines.

Fig. 1

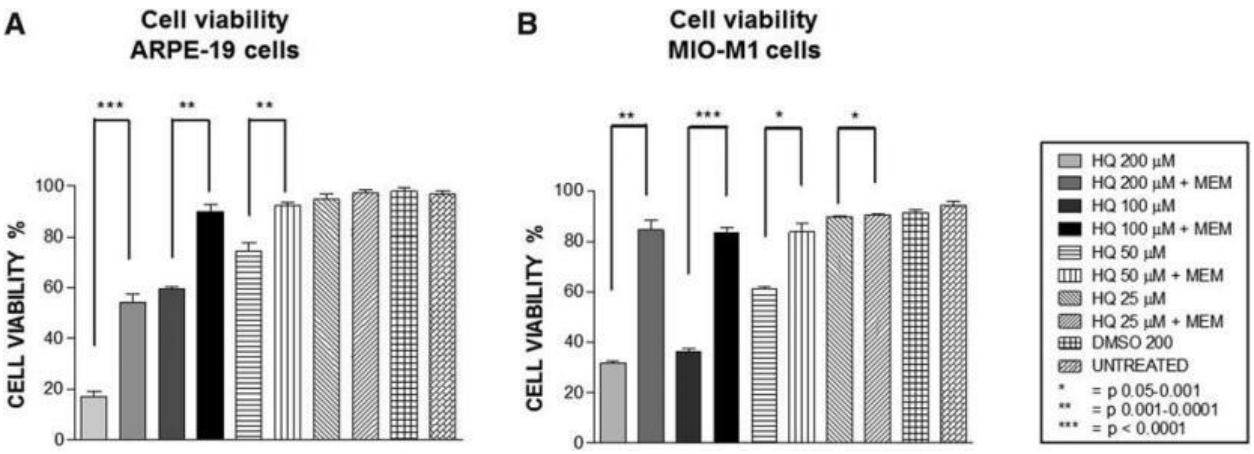
A
Cell viability
ARPE-19 cells
CELL VIABILITY %
B
Cell viability
MIO-M1 cells
CELL VIABILITY %
HQ 200 µM
HQ 200 µM + MEM
HQ 100 µM
HQ 100 µM + MEM
HQ 50 µM
HQ 50 µM + MEM
HQ 25 µM
HQ 25 µM + MEM
DMSO 200
UNTREATED
* = p 0.05-0.001
** = p 0.001-0.0001
*** = p < 0.0001

Fig. 2

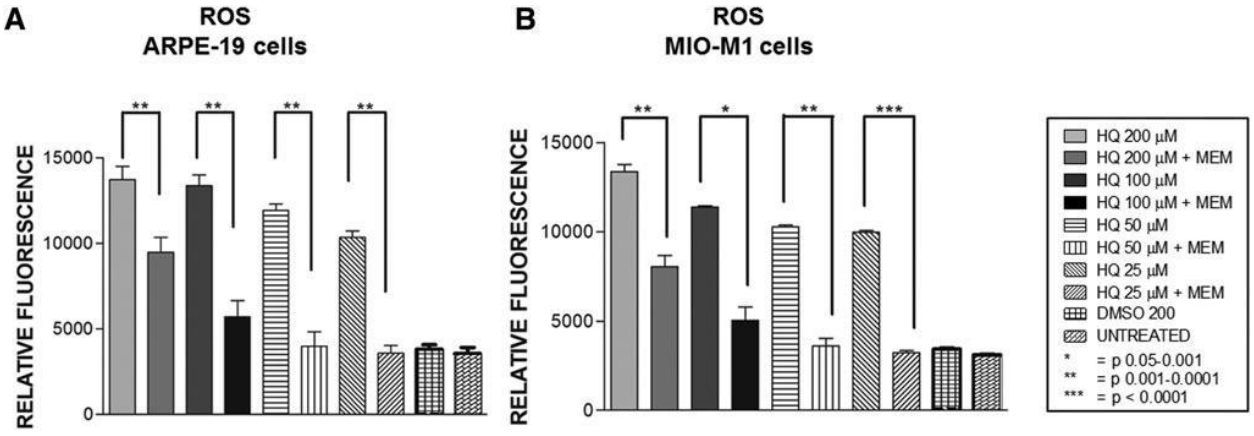
A
ROS
ARPE-19 cells
RELATIVE FLUORESCENCE
B
ROS
MIO-M1 cells
RELATIVE FLUORESCENCE
HQ 200 µM
HQ 200 µM + MEM
HQ 100 µM
HQ 100 µM + MEM
HQ 50 µM
HQ 50 µM + MEM
HQ 25 µM
HQ 25 µM + MEM
DMSO 200
UNTREATED
* = p 0.05-0.001
** = p 0.001-0.0001
*** = p < 0.0001

Fig. 3

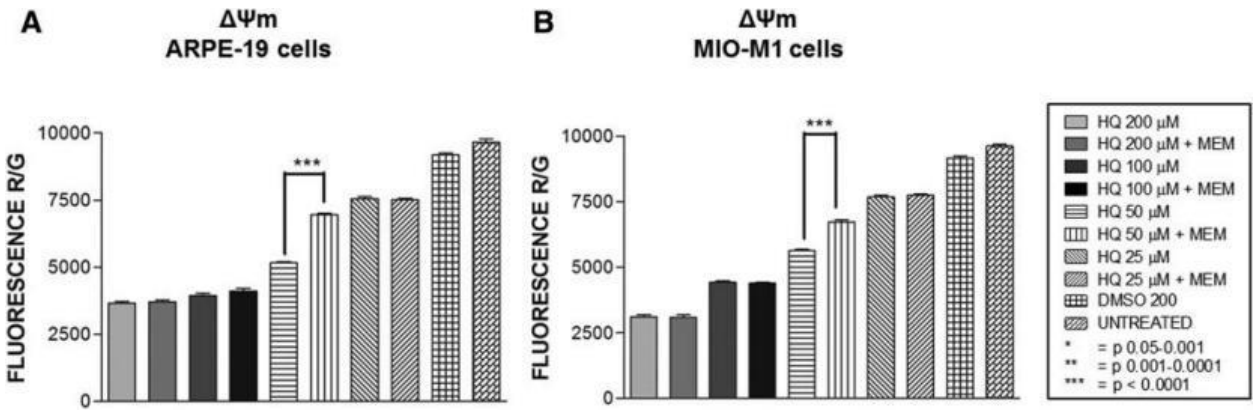
A
ΔΨm
ARPE-19 cells
B
ΔΨm
MIO-M1 cells
FLUORESCENCE R/G
10000
7500
5000
2500
0
***
HQ 200 µM
HQ 200 µM + MEM
HQ 100 µM
HQ 100 µM + MEM
HQ 50 µM
HQ 50 µM + MEM
HQ 25 µM
HQ 25 µM + MEM
DMSO 200
UNTREATED
* = p 0.05-0.001
** = p 0.001-0.0001
*** = p < 0.0001

Fig. 4

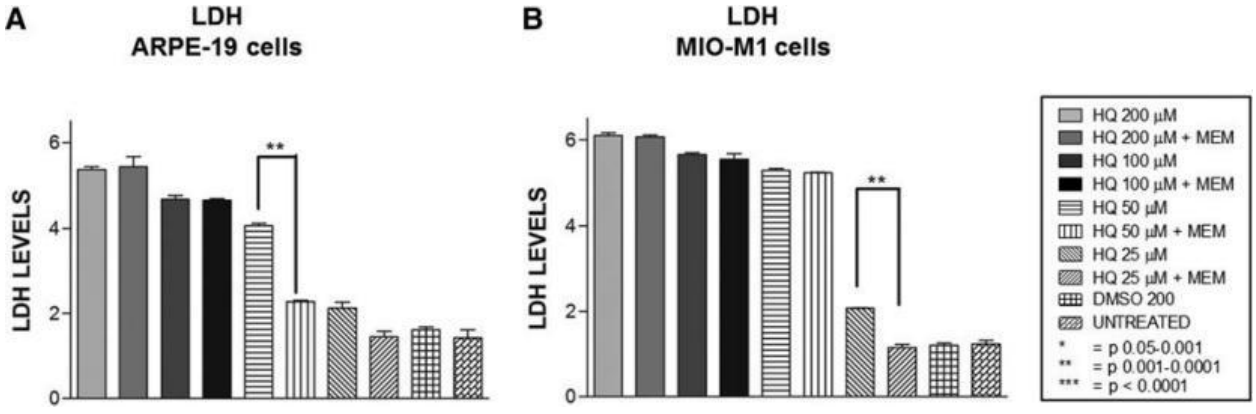
A
LDH
ARPE-19 cells
B
LDH
MIO-M1 cells
LDH LEVELS
6
4
2
0
**
HQ 200 µM
HQ 200 µM + MEM
HQ 100 µM
HQ 100 µM + MEM
HQ 50 µM
HQ 50 µM + MEM
HQ 25 µM
HQ 25 µM + MEM
DMSO 200
UNTREATED
* = p 0.05-0.001
** = p 0.001-0.0001
*** = p < 0.0001